Spectral shape-based assessment of SDOF nonlinear response to real, adjusted and artificial accelerograms.

Iunio Iervolino, Flavia De Luca*, and Edoardo Cosenza.
Dipartimento di Ingegneria Strutturale, Università degli Studi di Napoli Federico II, Naples, Italy.

ABSTRACT

The simple study discussed in this paper compared different procedures to obtain sets of spectral matching accelerograms for nonlinear dynamic analysis of structures in terms of inelastic seismic response. Six classes of records were considered: original (unscaled) real records, real records moderately linearly scaled, real records significantly linearly scaled, real records adjusted by wavelets, artificial accelerograms generated by two different procedures. The study is spectral shape-based, that is, all the considered sets of records, generated or selected, match individually (artificial and adjusted) or on average (real records) the same design spectrum for a case-study site in Italy. This is because spectral compatibility is the main criterion required for seismic input by international codes.
Three kinds of single degree of freedom (SDOF) systems, non-degrading and non-evolutionary, non-degrading and evolutionary, and both degrading and evolutionary, were used to evaluate the nonlinear response to the compared records. Demand spectra in term of peak and cyclic responses were derived for different strength reduction factors.
Results of the analysis show that artificial or adjusted accelerograms may underestimate, in some cases and at high nonlinearity levels, the displacement response, if compared to original real records, which are considered as a benchmark herein. However, this conclusion does not seem to be statistically significant. Conversely, if the cyclic response is considered, artificial record classes show a significant overestimation of the demand, which does not show up for wavelet-adjusted records.
The two classes of linearly scaled records do not show systematic bias with respect to those unscaled for both types of the response considered, which seems to confirm that amplitude scaling is a legitimate practice.

1 INTRODUCTION

Seismic assessment of structures via nonlinear dynamic analysis requires seismic input selection. Seismic codes suggest different procedures to select ground motion signals, most of those assuming spectral compatibility to the elastic design spectrum as the main criterion [1], for example Eurocode 8 [2], requires the average spectrum of the chosen set to be above 90% of the design spectrum in the range of periods 0.2T1 – 2T1, where T1 is the fundamental period of the structure. Practitioners have several options to get input signals for their analysis; e.g., real or real manipulated records and various types of synthetic and artificial accelerograms [3]. All these options are usually acknowledged by codes which may provide additional criteria or limitations for some of them. In the Italian seismic code [4], for example, artificial records, generated recurring to random vibration theory, should have duration of *at least 10s in their pseudo-stationary part*, and cannot be used in the assessment of geotechnical structures. Synthetic records, generated by simulation of earthquake rupture process, should refer to a characteristic scenario for the site in terms of magnitude, source-to-site distance and seismological source characteristics; finally real records should reflect the earthquake *dominating* the hazard at the site. However, practitioners not always can accurately characterize the seismological threat to generate synthetic signals or it is not possible to find a set of real records that fits properly code requirements in terms of a specific hazard scenario [5].
In fact, despite in the last decades the increasing availability of databanks of real accelerograms has determined a spread use of this type of records; it may be very difficult to successfully apply code

* Corresponding Author. Address: Dipartimento di Ingegneria Strutturale, Università degli Studi di Napoli Federico II, via Claudio 21, 80125 Naples, Italy. Tel +390817683672; Fax +39 0817683491. e-mail: flavia.deluca@unina.it

provisions to obtain code-compliant real record sets. In particular, provisions regarding spectral compatibility are hard to match if appropriate tools are not available [1,6]. This is why the relatively easy and fast generation of artificial records, perfectly compatible with an assigned design spectrum, is still very popular for both practice and research purposes.
More recently, procedures to get the spectral compatibility of real records by wavelets adjustment were proposed (e.g., [7]). This kind of manipulation is conceptually an extension of the more simple linear scaling of real records to modify (e.g., to amplify) the spectral shape to get a desired intensity level [8].
Although several studies tried to assess the *reliability* of each of these procedures (e.g., [9]), many of them are relatively narrow in scope without giving a general overview of the spectral compatibility issue. This work tries to address the spectral matching matter from the structural point of view in terms of ductility and cyclic response, having as reference a code-based design spectrum. To this aim six classes of 28 accelerograms, each of those comprised of four sets of 7, were considered: (1) unscaled real records; (2) moderately scaled real records; (3) significantly scaled real records; (4) wavelet-adjusted real records; (5) non stationary artificial records; (6) stationary artificial records. All sets are compatible with the elastic design spectrum for a case study in southern Italy.
The seismic responses of a large number of single degree of freedom (SDOF) systems, with different backbones, hysteretic relationships, and with various strength reduction factors (R), were considered. As structural response measures, or engineering demand parameters (EDPs), the ductility normalized with respect to the strength reduction factor and the equivalent number of cycles were considered to relate the ground motions to both peak and cyclic structural demand [10,11]. Analyses aimed at comparing the differences, if any, in the EDPs associated to each class of records with respect to the unscaled real records, considered as a benchmark. Hypothesis tests on selected samples were also carried out to assess the statistical significance of the results found in terms of both peak and cyclic response.

2 RECORD CLASSES

All the classes of records refer to the same 5% damped elastic design spectrum evaluated according the new Italian seismic code for a case-study site in Avellino (southern Italy, lat. 40.914, lon. 14.780). The spectrum considered is that corresponding to the life-safety limit state of an ordinary construction with a nominal life of 50 years on A-type soil class, according to Eurocode 8 classification; see [4] for details.
For each class four spectrum compatible sets, made of seven records each, were selected (if real) or generated (if artificial) because seven is the minimum sample to consider the average structural response as the design value according, among others, to the Italian and Eurocode 8 provisions. In the following the selection or generation processes are briefly reviewed, other information about the selection procedure can be found in [12].

2.1 URR - Unscaled real records

The sets of unscaled real ground motions (URR) were selected using REXEL 2.5 (beta), the software freely available at http://www.reluis.it/, which allows to select combinations of 7 records contained in the European Strong Motion Data Base (http://www.isesd.hi.is/) and the Italian Accelerometric Archive (http://itaca.mi.ingv.it/ItacaNet/), which on average match a code-based or user-defined elastic spectrum in a desired period range and with specified upper and lower bound tolerances [13]. Because REXEL can also automatically build the code spectrum for an Italian site based on its geographical coordinates, 4 sets of records were selected, each of those matching on average the target in the 0.15s-2.0s period range. Magnitude (moment magnitude, M_w) and source-to-site distance (epicentral, R_e) range between 5.6-7.8 and 0km-35km, respectively, site conditions are of A-type.

Because the Italian code design spectra approximate closely uniform hazard spectra provided for the Italian territory, initially the selection aimed at finding records with M_w and R_e equal to 5.8 and 14km, respectively; i.e., to the mean from disaggregation of peak ground acceleration (PGA) at the site[1] available at http://esse1-gis.mi.ingv.it/ (official Italian hazard data). However, due to the lack of spectrum matching unscaled real record sets fitting these restraints, M_w range had to be relaxed obtaining average values of magnitude and distance for the class equal to 6.5 and 15 km, respectively.

In Figure 1a the four sets are depicted along with the target spectrum. All the set averages are selected to be within [-10%, +30%] tolerance range with respect to the code spectrum, and in most of the compatibility interval they approximate very well the design spectral shape. To measure such an approximation the average deviation (δ), Equation (1), from the target spectrum may be introduced. In Equation (1) $Sa_{o,med}(T_i)$ represents the pseudo-acceleration ordinate of the average real spectrum corresponding to the period T_i, while $Sa_s(T_i)$ is the value of the spectral ordinate of the code spectrum at the same period, and N is the number of values within the considered range of periods (0.15s – 2.0s). All the URR sets have similar δ values; in fact: it is equal to 0.163 for set 1, 0.134 for set 2, 0.152 for set 3 and 0.141 for set 4. The 4 URR sets have no records in common and come from 17 different earthquakes, as it is shown in the Appendix (Table A1).

$$\delta = \sqrt{\frac{1}{N}\sum_{i=1}^{N}\left(\frac{Sa_{o,med}(T_i) - Sa_s(T_i)}{Sa_s(T_i)}\right)^2} \qquad (1)$$

In the following the SDOF response to various ground motion selection or generation methods will be compared referring to URR response. In fact, in this kind of studies it is necessary to define the "true" response (i.e., a point of comparison). Because the work herein presented is mostly aimed at comparing spectral matching in the light of code-compliant procedures, which often basically only prescribe the average spectrum of the set to match the design spectrum [1,5], the URR records are assumed as a benchmark. This means that if systematic difference in the response from another class of records with respect to URR will be found, this class will be considered "biased". However, this use of the *bias* term does not necessarily extends beyond this study as, in general, the URR may be not an unbiased baseline itself, even if allowed by the code, simply because, for example, selecting records that have a similar spectral shape, a selection bias can be created [15,16].

2.2 SF – Scaled real records

REXEL also allows selecting sets of seven accelerograms compatible with the reference spectrum if linearly scaled in amplitude. In other words, before the search, the spectra are preliminarily normalized dividing the spectral ordinates by the corresponding PGA. These non-dimensional spectra are compared to the target spectrum also normalized. Records belonging to spectrum matching combinations found in this way require to be linearly scaled to comply with the original code spectrum. Because REXEL allows controlling the average scaling factor (SF) of the combination, two classes of 4 scaled records sets each, (i) SF equal to 5; (ii) and SF equal to 12, were selected from A-type site class accelerograms. The intent is to compare response to records moderately and significantly scaled.

[1] It is to recall here that, more accurately, disaggregation to be matched should be that for the hazard of the spectral ordinate at the fundamental period of the structure [14].

2.2.1 SF5

In the same range of periods in which there is spectral compatibility (0.15s – 2s), with the same tolerances, and in the same magnitude and distance intervals chosen for URR, 4 set of 7 compatible accelerograms, each of those having a mean SF equal to 5, were selected, Figure 1b.
The 28 records (9 records in common with URR) come from 15 earthquake events (10 of them are in common with URR), as shown in Appendix (Table A2).
In this case the deviations of the sets are smaller than URR records' deviations, as expected [1,6], being equal to: 0.082 for set 1, 0.087 for set 2, 0.069 for set 3 and 0.089 for set 4.

2.2.2 SF12

Using REXEL also 3 sets of 7 records whose mean SF was 12, were selected, each of those matching on average the target in the 0.15s-2.0s period range. Magnitude and source-to-site distance range between 5.5-7.8 and 0km- 50km. Because it was not possible to find another set with the desired characteristics via REXEL, the fourth set of seven accelerograms was "manually" selected in the same magnitude and distance ranges so that its deviation and its average scaling factor were similar to the other three software-aided selected sets, Figure 1c.
These four sets have no events in common with the URR class and belong to 17 different earthquakes, as shown in Appendix (Table A3). In this case, deviations of the sets are still smaller than deviations of URR and comparable to deviations of the SF5 sets, being equal to: to 0.072, 0.078, and 0.117 for the software selected sets and equal to 0.207 for the manually selected set, respectively.

2.3 RSPMatch - Wavelet adjusted records

RSPMatch2005 software[2] [17,7], was used to modify the URR accelerograms. Spectral matching software, as RSPMatch2005, make adjustments to recorded ground motions to provide a good match with a target response spectrum. Using spectrally-matched records as an input to time-history analysis helps to reduce the variability in the seismic demand, and therefore allows fewer records to be used to obtain stable estimates of the expected response [15]. Generally, RSPMatch2005 is able to provide an excellent match of the target spectrum across a wide range of periods (and, if required, at multiple damping levels), with relatively small adjustment to the seed accelerogram. Useful guidelines and reliable selecting criteria to choose set of records suitable to be adjusted by the software can be found elsewhere (e.g., [18]).
In this case the adjustment procedure was simply aimed at reducing dispersion of records, in a specific period range, with respect to the target. The procedure was pursued only for the 5% damping factor in the range of periods 0.15s-2.0s in which records were already compatible on average, Figure 1d.
It is to note that wavelet adjustment was applied in a relatively limited period range. Nevertheless, even if the matching in the 0.15s-2.0s interval produced individual spectrum modification also beyond that range (Figure 1d), the average of RSPMatch class is close to the target also in the 2s-4s range.

2.4 Artificial records

Generally speaking, generation procedures for artificial accelerograms are based on the random vibration theory and the spectral matching is carried out iteratively adjusting the Fourier amplitude spectrum of each accelerogram generated [19]. In this way, spectral matching procedures are carried out in the frequency domain by the use of a power spectral density function, the selection of which is the key issue and represents the main difference between various generation procedures.

[2] Courtesy of Damian Grant, ARUP, USA.

The software considered in this study generate different kind of signals: the first one, Belfagor [20] produces non stationary signals based on the semi-empirical method of Sabetta and Pugliese [21]; the second one SIMQKE [22] produces stationary signals that are subsequently enveloped in a trapezoidal shape to roughly simulate non-stationary characteristics of ground motion.

2.4.1 Belfagor sets

Belfagor (http://www.unibas.it/utenti/mucciarelli/index.html) generates non stationary signals by using variable Fourier amplitudes empirically evaluated from the Sabetta and Pugliese ground motion prediction equation [21]; in fact, the code asks for reference M_w, R_e, and soil type. Because of record's non-stationary character, these parameters influence strictly the shape of the signal even if the spectral matching procedure is based on a smooth code spectrum.
A class of 28 accelerograms was generated for the purposes of this study. The input M_w and R_e values for each signal were equal to those of the URR and *stiff soil type*, according to [21], was assumed. All the generated records have the same duration, 21.48s with a 0.005s time step (default values of Belfagor). The duration is slightly lower than the minimum prescribed by the Italian code for artificial records (25s); however this 15% difference is not believed to affect results (see also section 2.5).
Although not strictly necessary for the purposes of this study, the accelerograms were randomly arranged in four sets of seven consistently with the other classes, Figure 1e.

2.4.2 Simqke sets

A second class of artificial records was generated by Simqke (http://bsing.ing.unibs.it/~gelfi/software/simqke/). This is the commonly used method for generating synthetic ground motions, which are compatible with a prescribed design spectrum. This method is based on simulation of stationary processes. The matching of the target spectrum may be improved by means of an iterative procedure. Other studies evaluated the influence of iterative option in the software that was not considered in this case (e.g., [9]).
In this case 28 records were generated in a single run of the software and subsequently they were separated in 4 groups of 7, Figure 1f. They fully respect the Italian code's provisions in terms of duration of both stationary and non-stationary parts. In fact, as it was reported previously, this software simulates record non-stationary by enveloping the signal obtained in a trapezoidal shape, and the user can choose how long to make the beginning and ending of non stationary part.

2.5 Integral ground motion parameters

Each accelerogram of the six classes was processed to evaluate its characteristic other than the spectral shape, in particular in terms of integral intensity measures (IMs). Average values of Arias intensity (I_A), Equation (2), and of Cosenza and Manfredi index [23] (I_D), Equation (3), computed as the average on the sample of 28 records for each class, are reported in Figure 2. In Equation (2) and (3) a(t) is the signal's accelerometric time-history, whose duration is equal to t_E, and PGV represents the peak ground velocity.

$$I_A = \frac{\pi}{2 \cdot g} \int_0^{t_E} a^2(t)\, dt \qquad (2)$$

$$I_D = \frac{2 \cdot g}{\pi} \frac{I_A}{PGA \cdot PGV} \qquad (3)$$

It seems that the Simqke generation process is not able to reproduce characteristic Arias intensities of real events at least if compared to URR, SF5, and SF12. Scaled real records have lower I_A values, on average, with respect to the URR as well as those adjusted via RSPMatch2005. However, when passing to I_D, which is supposed to be better related than I_A to structural cyclic response expressed in terms of equivalent number of cycles [11], both scaled and unscaled real records and RSPMatch

have close average values of I_D. Both classes of artificial signals display higher values of I_D, especially the Simqke accelerograms because of the high I_A.
Also the significant duration (Sd), defined as the time interval between 5% and 95% of I_A accumulation, was computed. Table 1 reports average values of Sd for each class. Only Simqke records show duration clearly larger than others.

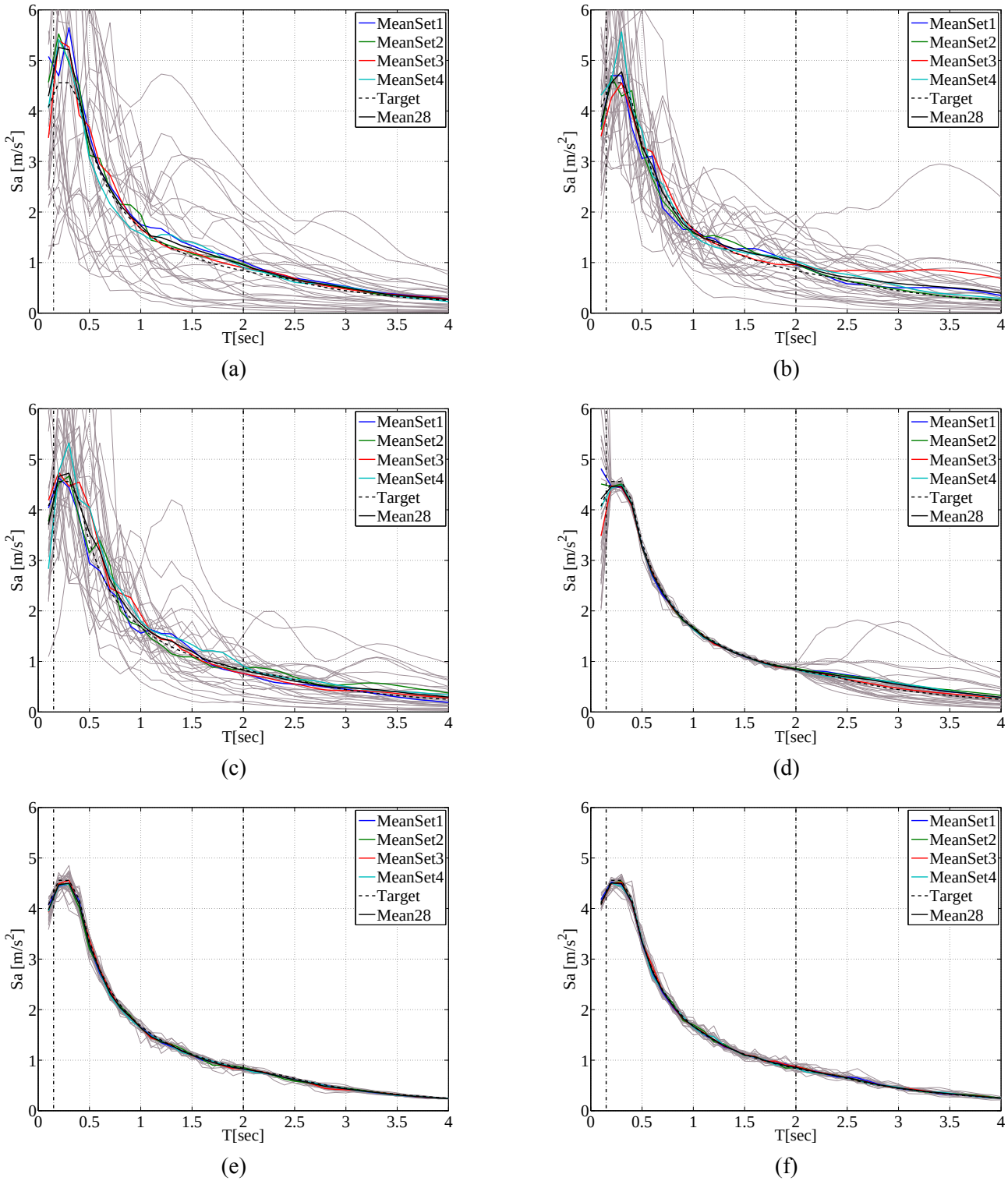

Figure 1. URR (a), SF5 (b), SF12 (c), RSPMatch (d), Belfagor (e), and Simqke (f) acceleration elastic spectra, compared to the target spectrum.

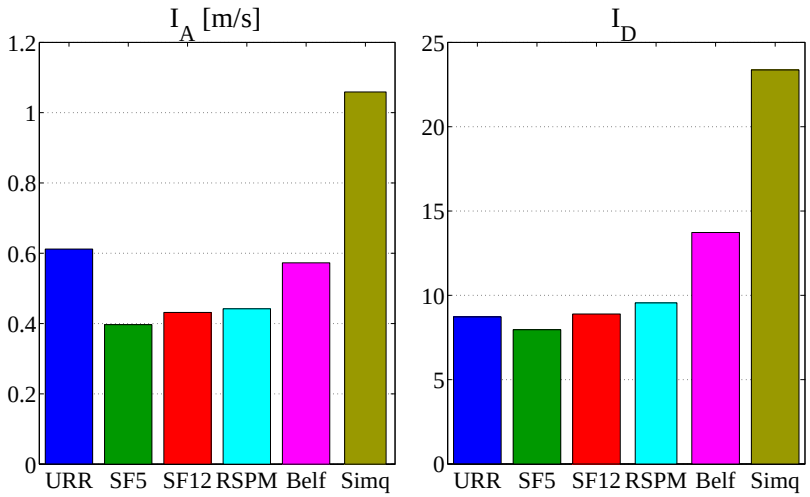

Figure 2. Average values of I_A and I_D for the considered classes of records.

Table 1 Average values of Sd for the considered classes of records.

URR	*SF5*	*SF12*	*RSPM*	*Belf*	*Simq*
13.7s	*12.5s*	*10.4s*	*13.8s*	*12.0s*	*18.0s*

Although it was discussed how integral parameters such as I_D are good IMs for cyclic response, one may argue that the correct value to match is not necessarily that of URR. To investigate this, in Figure 3 the probability of exceedance of I_D conditional to the PGA of the target spectrum is reported for three M_w-R_e pairs. The first pair chosen (M_w=5.0 and R_e=5.0km) is the modal pair from disaggregation of the hazard for the design PGA at the site, the second pair (M_w=5.8 and R_e=14.0km) is the mean. For comparative purposes, a third couple of M_w and R_e (M_w=6.5 and R_e=15.0 km) was considered, it represents mean M_w and R_e of the URR class. The curves in Figure 3 were obtained via *conditional hazard analysis* according to the procedure[3] described in [24] and [25].

The mean I_D of all the classes of records can be compared with the I_D distributions. It may be observed that the likely I_D values given the PGA at the site are 5.3 and 7.2 as median, 3.5 and 4.7 as 16% and 8.2 and 11.1 as 84% percentile, respectively for the mode and mean M_w and R_e from disaggregation. URR mean M_w and R_e give 5.3, 8.3 and 12.8 as 16%, 50% and 84% percentiles respectively.

All the three complementary cumulative distributions of I_D suggest that the artificial signals are characterized by unusual integral parameters although matching the same elastic spectrum of all the other record classes.

[3] As discussed in [24] and [25] the conditional I_D distribution would require to account for all M_w and R_e pairs weighted by their contribution to hazard from disaggregation and this would be the "exact" result in terms of the distribution of integral ground motion features given the design peak acceleration. However, a simplified and approximated approach may be followed using only representative pairs form the joint M_w and R_e disaggregation distribution. This approach is also used herein; different representative pairs lead to slightly different (approximated) results.

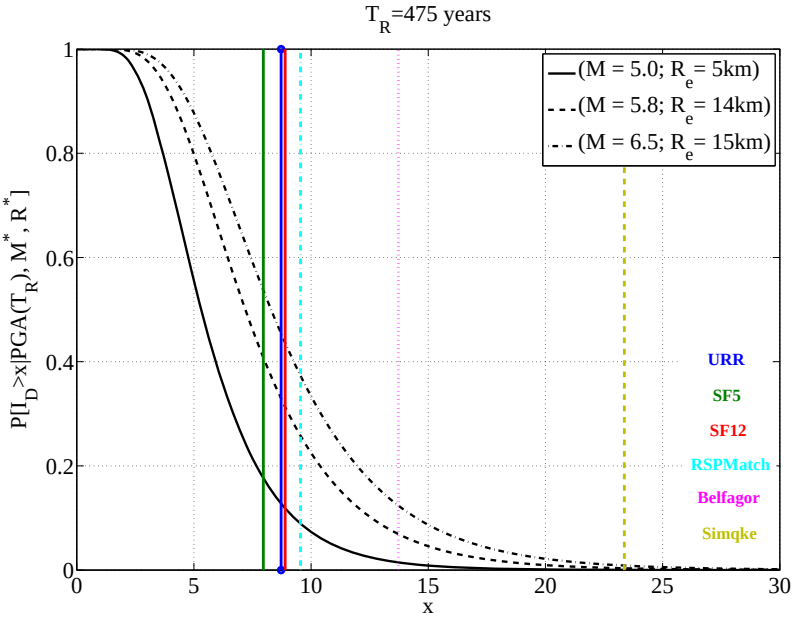

Figure 3. Comparison between probability of exceedance of I_D conditional to the PGA value of the target elastic spectrum and I_D medium values of each record category.

3 SDOF SYSTEMS AND DEMAND MEASURES

All records selected for each class were used as input for nonlinear dynamic analyses applied to 240 SDOFs. They belong to three classes of hysteretic behavior with elastic period varying from 0.1s to 2s, sampled with 0.1s step. Elastic-plastic with hardening (EPH) SDOF represents non-degrading and non-evolutionary structures. The post-yielding stiffness was assumed as 0.03 of the initial stiffness (k_{el}), Figure 4a. The second class of inelastic SDOFs has a non-degrading and evolutionary relationship; its backbone is elastic perfectly plastic (EPP) and it is characterized by a degrading stiffness; Clough and Johnston model [26] was considered (Figure 4b). The third class of inelastic SDOFs has a softening backbone (ESD); a Takeda hysteretic rule was assumed [27]. The softening stiffness is equal to 10% of the elastic one and 10% of yielding strength was taken as the residual value. All ESD systems have ductility before reaching the residual strength, evaluated as the ratio between ultimate displacement (Δ_u) and yielding displacement (Δ_y) in the backbone curve, equal to 10. In the following, this ductility value will be called *ductility limit*, Figure 4c. In all panels of Figure 4, F_y is the yielding strength of the SDOF.

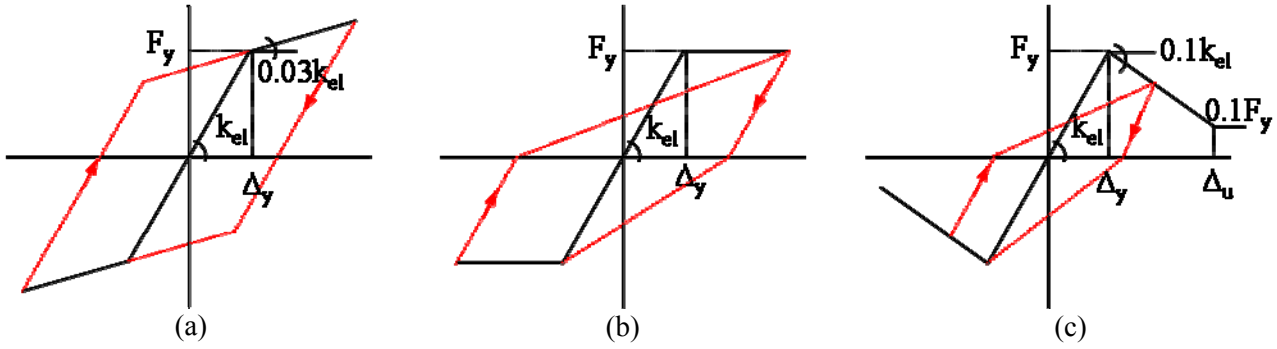

Figure 4. EPH backbone curve (a), EPP backbone curve (b), ESD backbone curve (c).

To have a response that ranges from mildly inelastic to severely inelastic, for all SDOF systems four strength reduction factors (R) were considered: 2, 4, 6 and 10. Note that the peak deformation experienced by an elastic structure is a ground motion specific quantity. Therefore, one can achieve the same value of R either for each record in a dataset (*constant R approach*) or on an average sense

(*constant strength approach*) keeping constant the yielding strength. The latter was adopted in this case, to simulate the effect of different sets of accelerograms on the same structure (same F_y value at a given oscillation period T), given the design spectrum. However, it should be emphasized that the two different approaches can lead to different conclusions as pointed out by some authors (e.g., [28]).

3.1 Engineering demand parameters

EDPs chosen were selected to investigate both peak and cyclic seismic response. Displacement-based parameters is the ratio between displacement ductility and reduction factor (D_{kin}/R), the former evaluated as the ratio of the peak inelastic displacement ($Sd_{R=i}$) and yielding displacement, according to Equation (4).

$$D_{kin} = \frac{Sd_{R=i}}{\Delta_y} \tag{4}$$

The cyclic response-related parameter is the equivalent number of cycles (N_e). This latter parameter is given by the cumulative hysteretic energy (E_H), evaluated as the sum of the areas of the hysteretic cycles (not considering contribution of viscous damping), normalized with respect to the largest cycle, evaluated as the area underneath the monotonic backbone curve from the yielding displacement to the peak inelastic displacement ($A_{plastic}$), Equation (5). This allows separating ductility demand (already considered above in D_{kin}) and cyclic demand [11].

$$N_e = \frac{E_H}{A_{plastic}} \tag{5}$$

4 RESULTS AND DISCUSSION

4.1 Elastic displacements and ratio to the target code spectrum

Elastic displacement spectra, evaluated as mean value on 28 records for each class, are compared to the target spectrum transformed from pseudo-acceleration, Figure 5a.
Figure 5b reports the ratio of the average spectrum of the class and the code spectrum, that is, the deviation of each class (Sd_{el}) with respect to the target spectrum ($Sd_{el\text{-}target}$), as it may help to understand the nonlinear results presented in the following. Although all classes are spectrum matching, real records spectra show the largest deviation with respect to the target, as it was anticipated. This is because real records match the target on average, while for the other three classes (adjusted and artificial records) each single records matches closely the target (see Figure 1). From Figure 5b it is possible to recognize that all the average spectra of the six record classes selected are above 90%, and mostly below 20%, of the target in the 0s-4s range. This renders the classes suitable, according to Eurocode 8 spectral matching provisions, for structures with a fundamental period up to 2s.

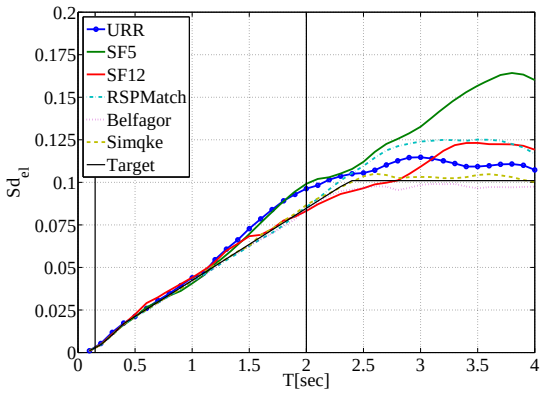

(a)

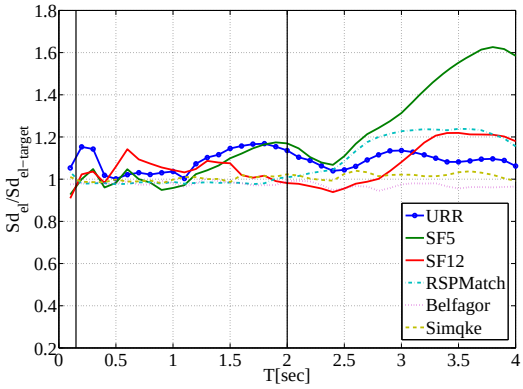

(b)

Figure 5. Average values of elastic displacement (a) and ratio to the target spectrum for the record classes (b).

4.2 Ductility demand

Figure 6 shows ductility demand normalized with respect to the different R values investigated referring to the EPH system. For low R, normalized ductility seems to be similar for all six classes of records. The cases for high R values (Figure 6c and Figure 6d) emphasize an apparent underestimation of ductility for artificial records with respect to real records classes. In particular, results for R equal to 10 show different underestimation levels for adjusted and artificial classes of records: Belfagor class is followed by Simqke and RSPMatch. Ductility response indicates that wavelet adjusting procedure gives a lower bias. On the other hand, it should be recalled that RSPMatch records are the same records as URR to which the adjustment procedure was applied. Linearly scaled records, indifferently if moderately or significantly, seem to show no trends with respect to URR. Although, the large scattering of real records with respect to the target, leads to large variability of the average estimated response from class-to-class of real records; e.g., Figure 6c and Figure 6d.

Figure 7 shows normalized ductility results for EPP systems. The stiffness degrading behavior of these SDOFs tends to confirm conclusions found for EPH systems. However, when interpreting the results for these two backbones it should be recalled that URR class had a linear demand which was already generally above that of the artificial records. Moreover, hypothesis tests, (to follow), do not confirm these differences to be statistically significant.

Figure 8 shows normalized kinematic ductility demand for ESD systems; in this case the trends are less clear. For R factors up to 4 it is possible to recognize about the same trends found for EPH and EPP systems, see Figure 8a and Figure 8b, with some underestimation of nonlinear demand that is systematically about 100%, for artificial and adjusted records with respect to real records classes. For higher R values (6 and 10), see Figure 8c and Figure 8d, it is not possible to recognize the same trends; all classes except Simqke records, show similar ductility demands. This has an explanation related to modeling of the nonlinear systems; in fact, for R equal to 6 and 10 the ESD SDOFs exceed the *ductility limit* and start cycling on the residual strength branch of the backbone. This behavior which is systematic for all record classes has a smoothing effect on the differences among the classes of accelerograms. However, it seems to be confirmed also for ESD systems that SF5 and SF12 classes do not show any trend with respect to URR.

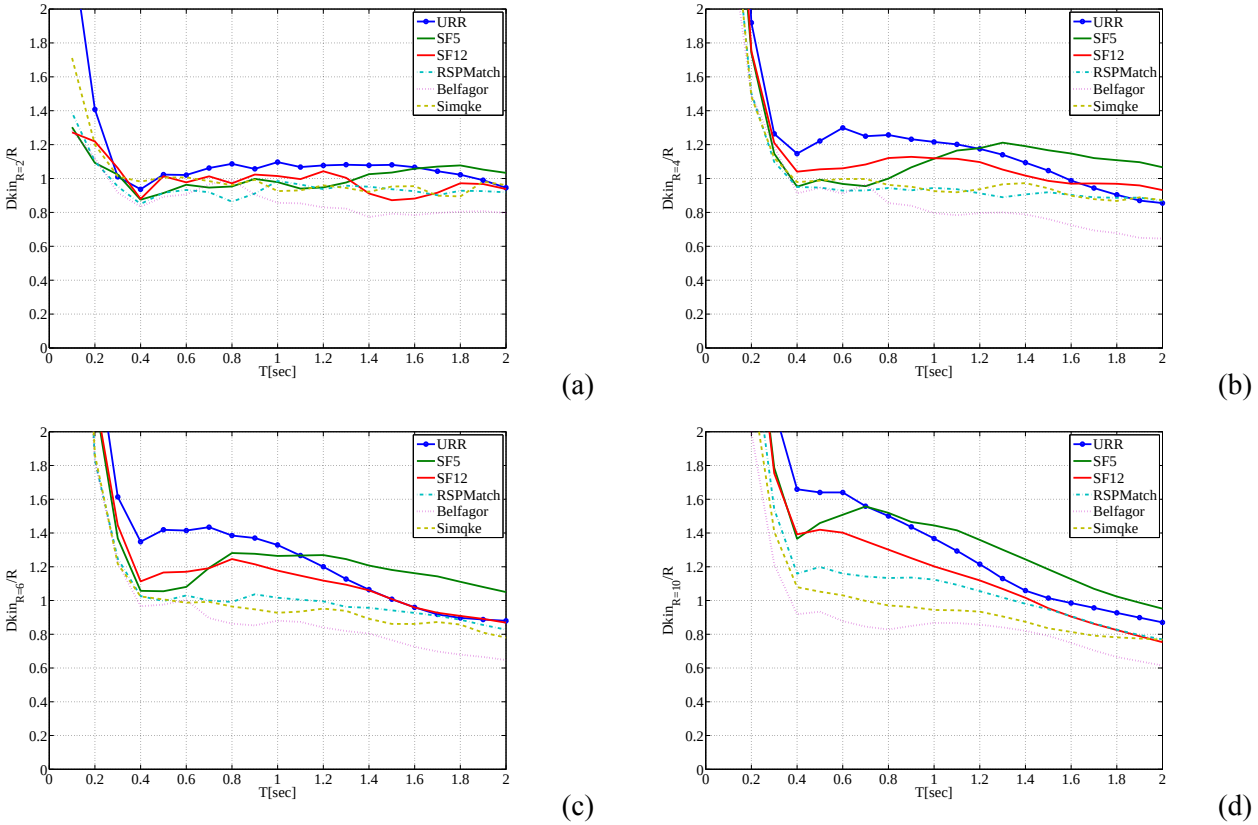

Figure 6. Average values of ductility demand for EPH system computed as mean value of 28 records.

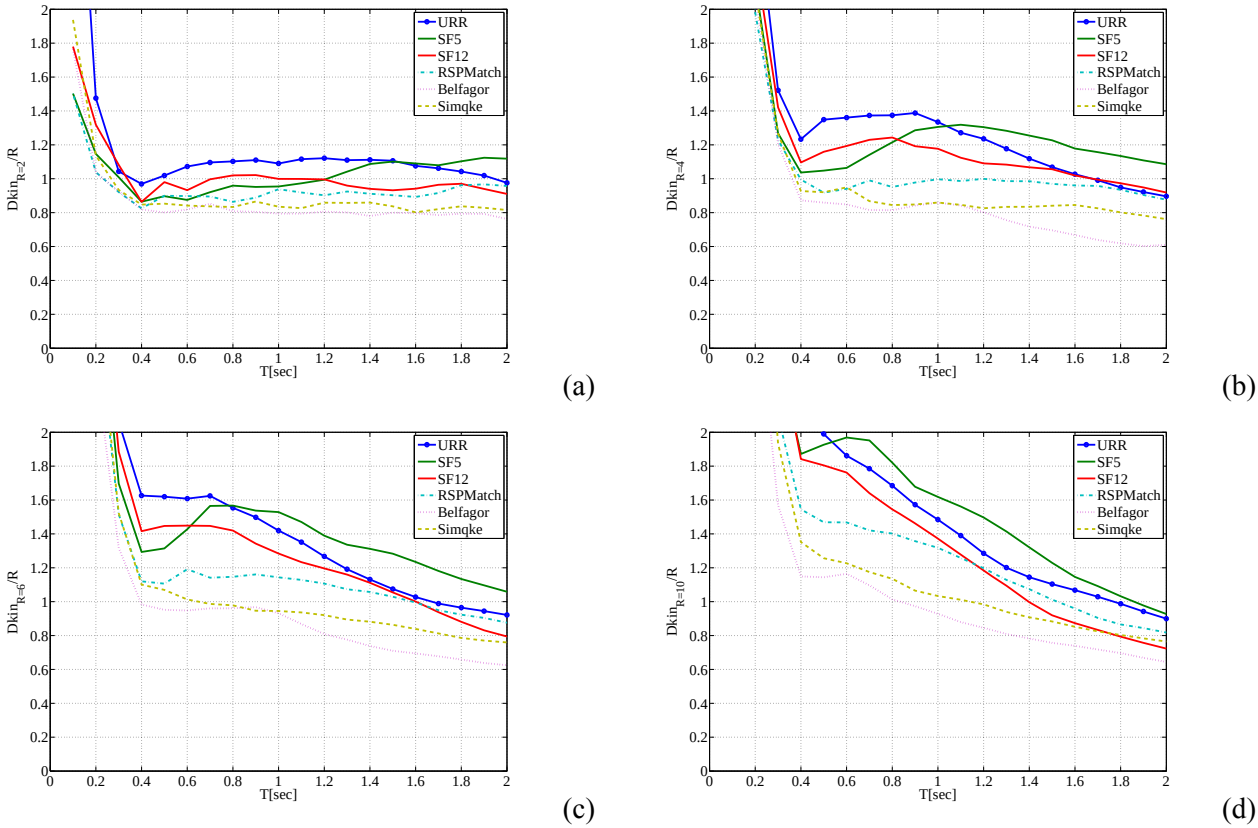

Figure 7. Average values of ductility demand for EPP system computed as mean value of 28 records.

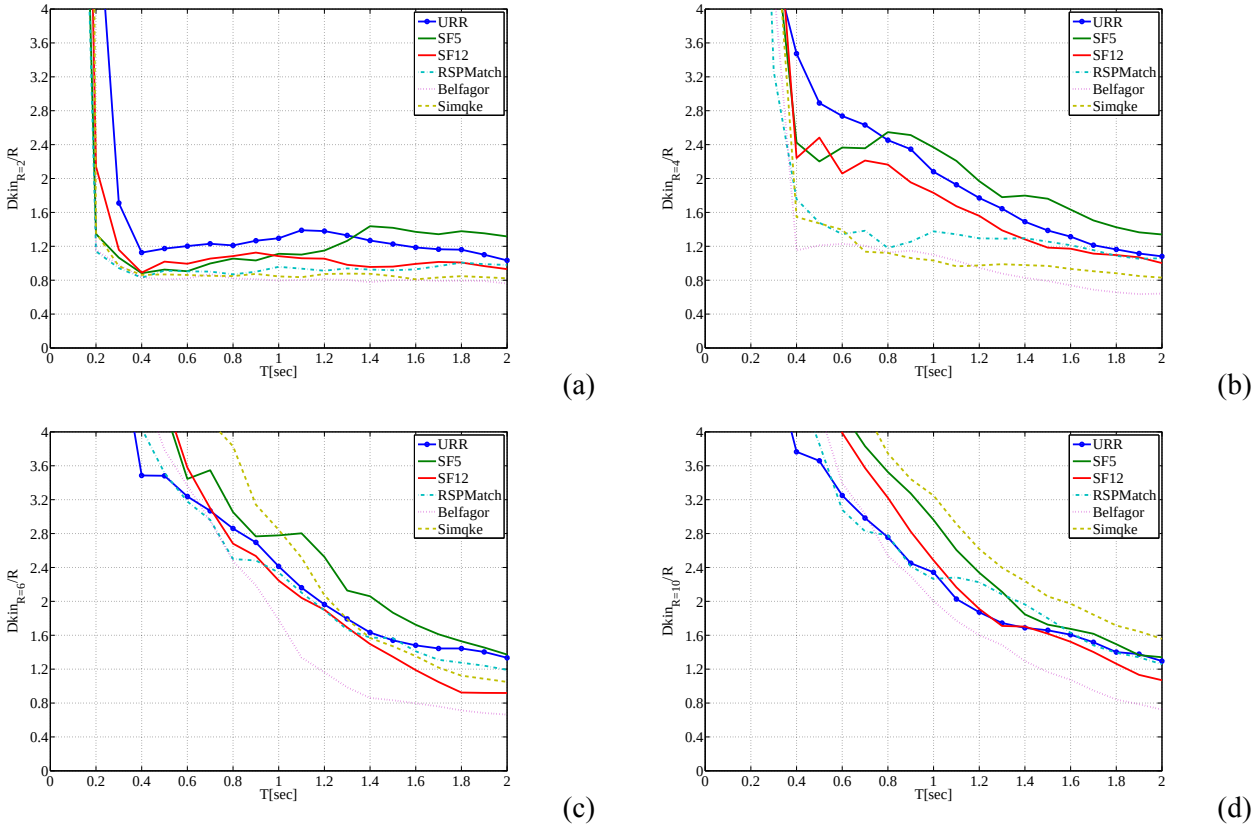

Figure 8. Average values of ductility demand for ESD system computed as mean value of 28 records.

4.3 Equivalent number of cycles

N_e has the mentioned advantage of normalizing cyclic response with respect to peak demand, Equation (5), allowing a comparison between the different classes of records in terms of cumulative demand only. Figure 9 shows the values of this EDP for the EPH systems at different R values. For all the R investigated a strong overestimation in term of cyclic response may be observed for both classes of artificial records. Simqke records show the highest overestimation (e.g., twice than URR at low periods). Belfagor results shows that a generation procedure based on non-stationary characteristics of the earthquake gives more acceptable results in terms of cyclic response. Cyclic EDP results seem to be independent of strength reduction factor, at least for R values ranging from 4 to 10.The latter is an expected result, in fact, N_e represents the total hysteretic energy normalized with respect to energy of the maximum cycle.

SF5 and SF12 records have, again, a non systematic trend with respect to URR, confirming that scaling procedure does not introduce any bias even if the scaling factor is large. RSPMatch records give results very close to URR indicating that the wavelet adjustment does not influence the cyclic response.

Figure 10 shows the N_e results for the EPP systems. The same conclusions found for EPH systems hold. In this case the lower reduction factors (2,4) are characterized by the largest N_e, this effect is strictly related to a decrease in the total hysteretic energy with the strength reduction factor.

Figure 11 shows N_e for ESD systems. Again, the same trends found for EPH and EPP hold. Artificial records show cyclic response overestimation, while wavelet adjustment seems to introduce no bias with respect to URR. Moderately and significantly scaled real records also show no trends. Note that, for large strength reduction factors (6,10), N_e tends to be similar for all classes. This is because ESD systems, at high nonlinearity level, easily reach the residual strength branch of the backbone.

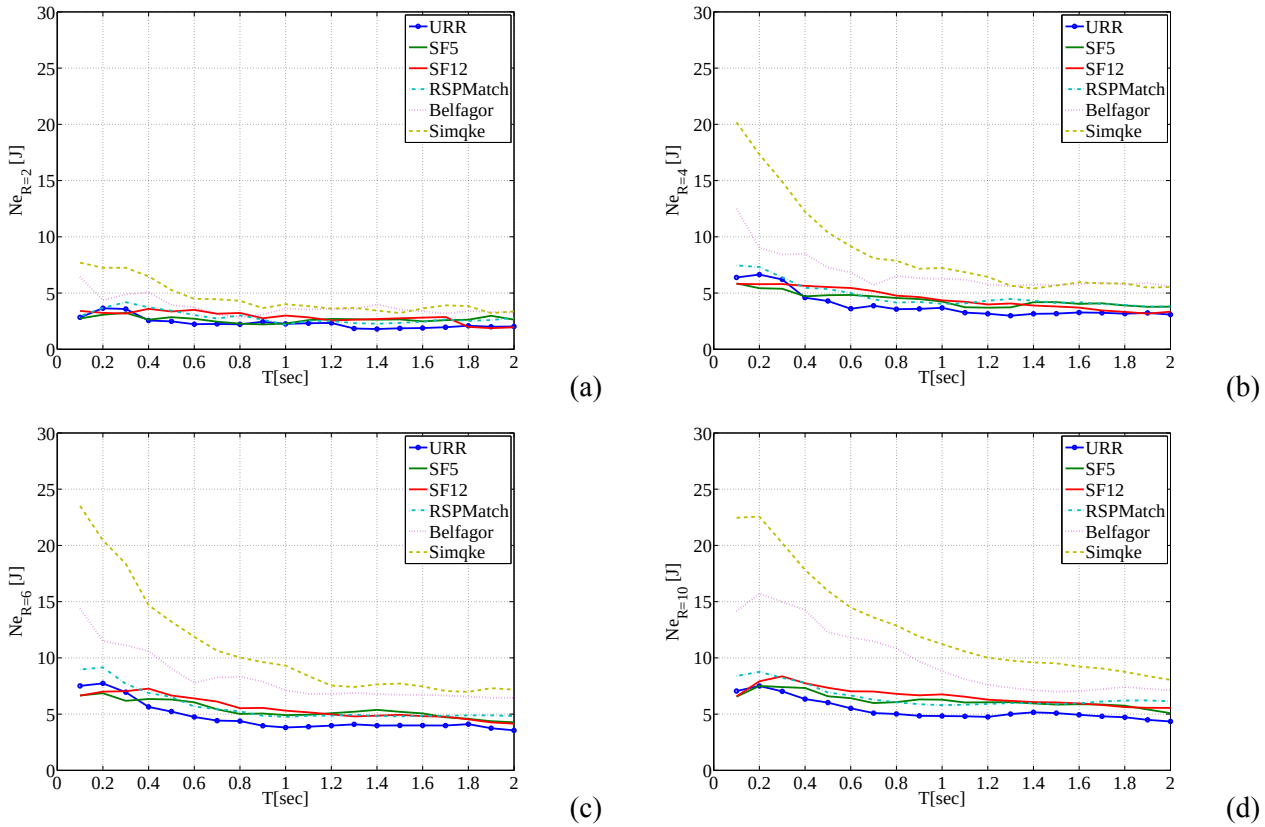

Figure 9. Average values of equivalent number of cycles for EPH system computed as mean value of 28 records.

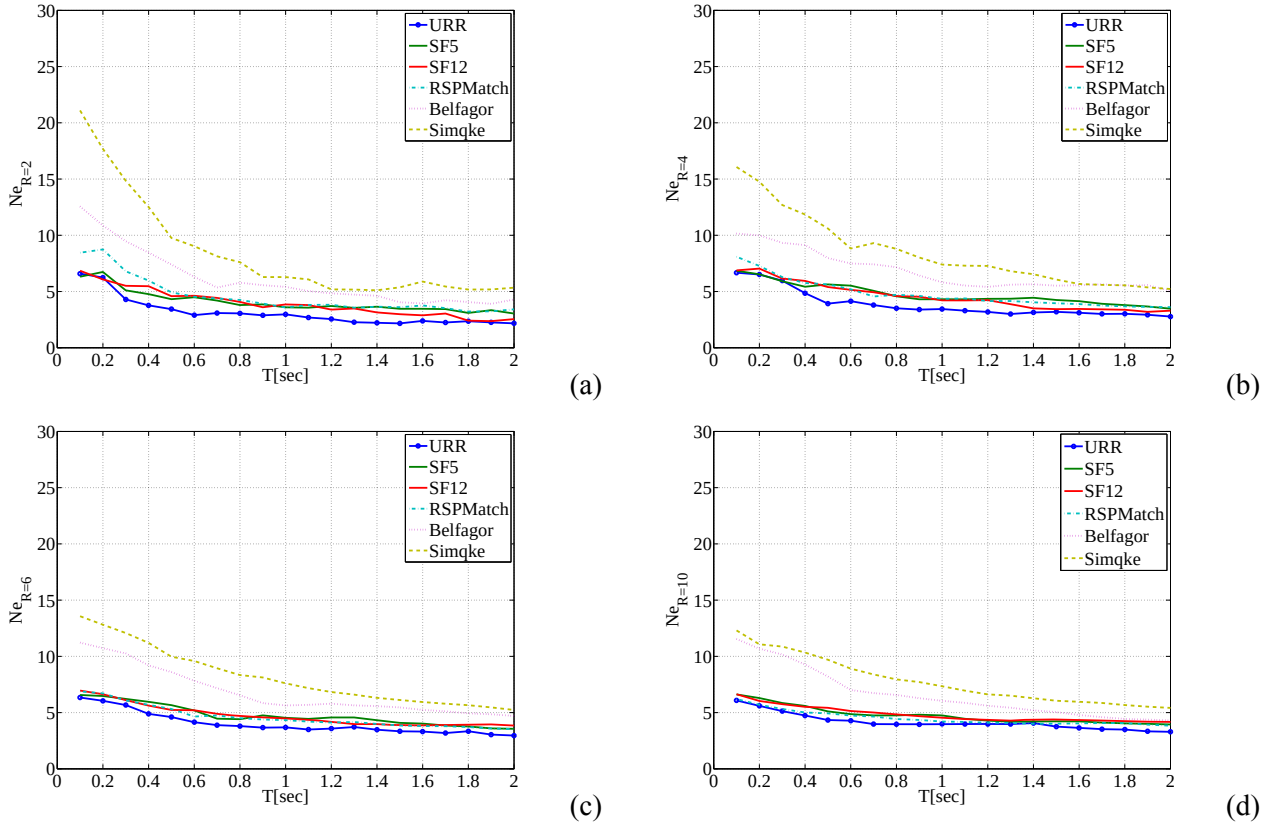

Figure 10. Average values of equivalent number of cycles for EPP system computed as mean value of 28 records.

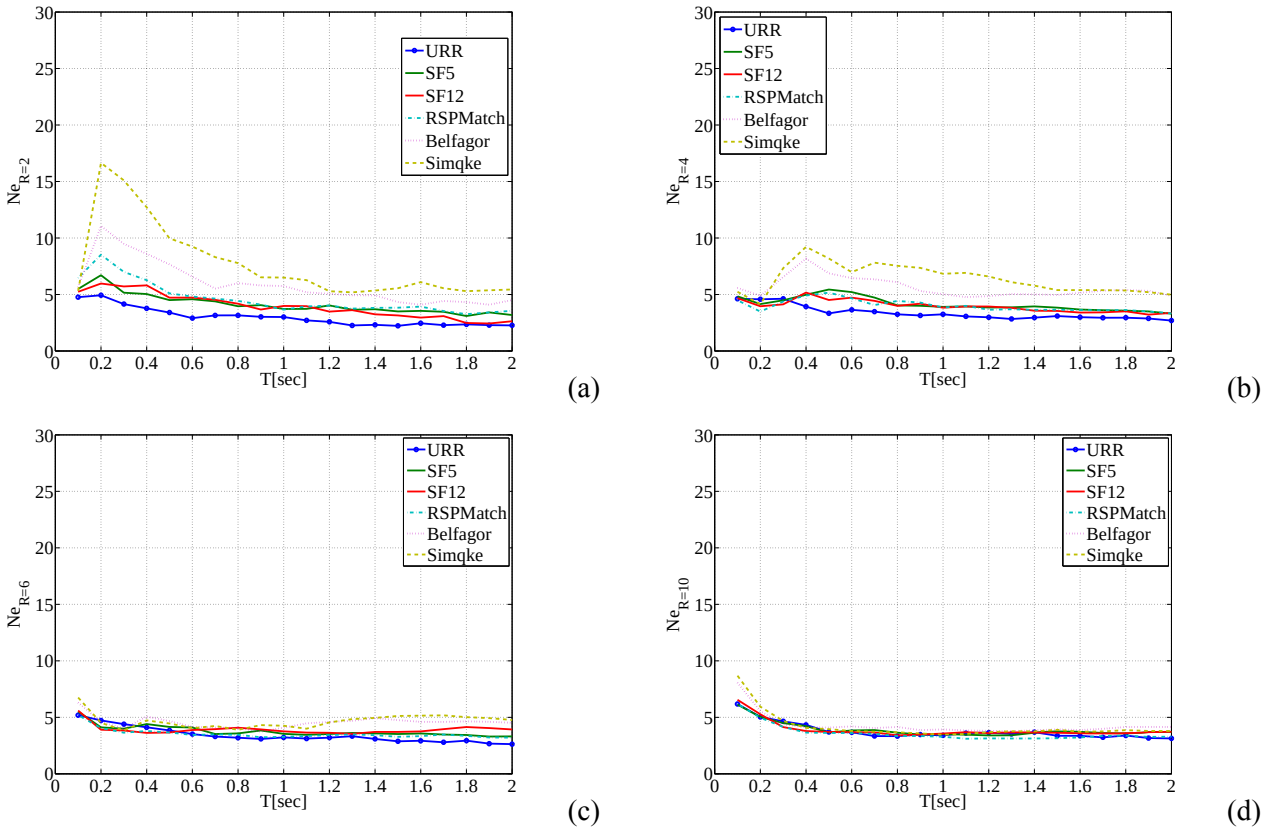

Figure 11. Average values of equivalent number of cycles for ESD system computed as mean value of 28 records.

4.4 Prediction of cyclic response

Cyclic response overestimation of artificial records was a predictable result; in fact artificial records are characterized by higher values of integral parameters, especially I_D. Figure 12 shows, as an example, the I_D versus N_e plot of each record for EPH systems with R equal to 4, at two periods equal to 0.6s and 1.0s, Figure 12a and Figure 12b, respectively. Figure 13 shows I_D versus N_e plot for EPP system characterized by the same R at the same periods of Figure 12. Similarly to EPH systems, it is possible to note a fairly good correlation between the two parameters. Figure 14 refers to ESD systems, in this case the correlation is still good but become less recognizable for higher R values due to fact that at these nonlinearity levels the *ductility limit* of the degrading system does not emphasize differences between equivalent number of cycles response of each class (i.e., Figure 11c and Figure 11d).

As a conclusion, considering I_D evaluated in section 2.5 for all records classes, and their compliance with the conditional hazard analysis, the latter can be suggested as an additional criterion in selection or generation procedures for accelerograms when the cyclic response represents a critical performance parameter for the structure to be analyzed.

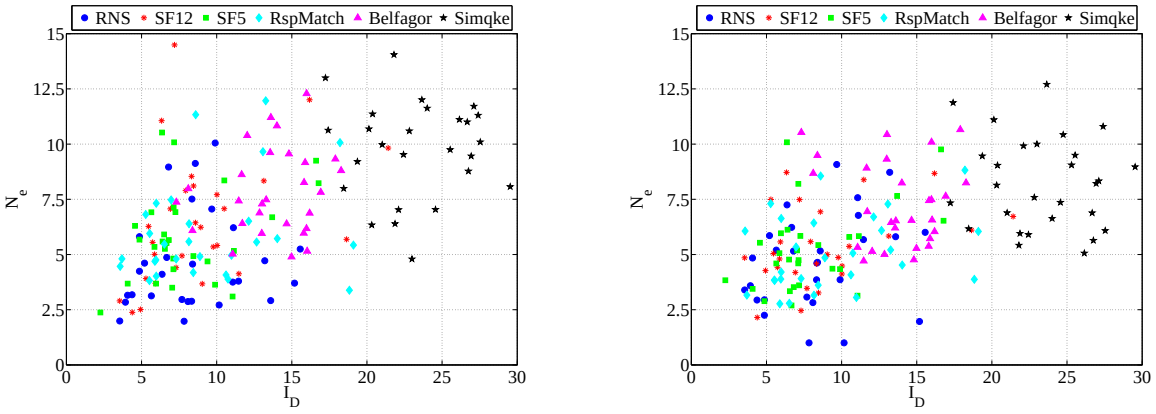

Figure 12. N_e versus I_D for R = 4 and T = 0.6s (a) and T = 1.0s (b) evaluated for system EPH for each record of each class.

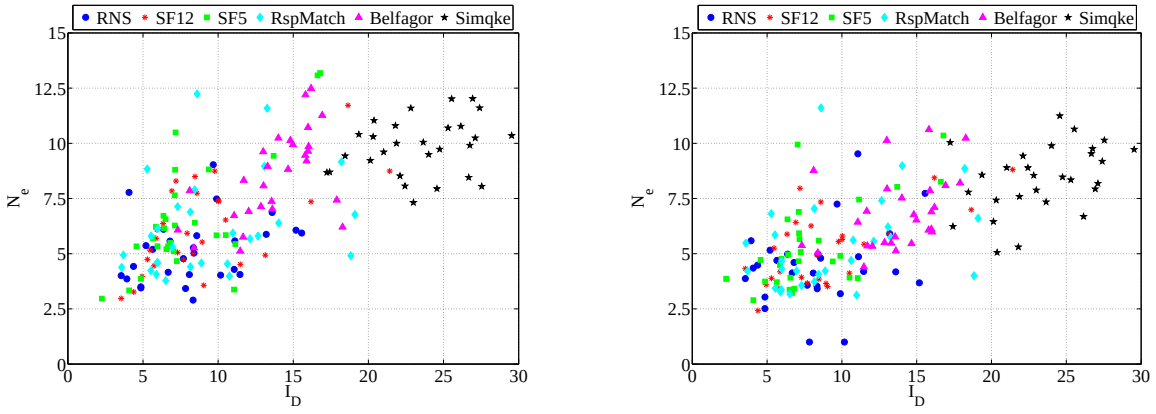

Figure 13. N_e versus I_D for R = 4 and T = 0.6s (a) and T = 1.0s (b) evaluated for system EPP for each record of each class.

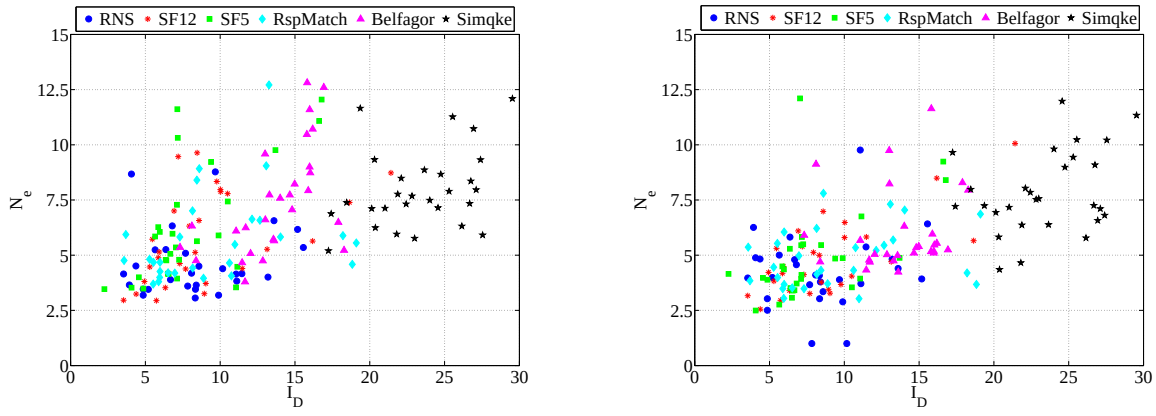

Figure 14. N_e versus I_D for R = 4 and T = 0.6s (a) and T = 1.0s (b) evaluated for system ESD for each record of each class.

5 HYPOTHESIS TESTS

To finally draw conclusions from the results above, it may be helpful trying to quantitatively assess their significance. In particular, parametric hypothesis tests [29] were performed to assess to what significance the median values of the response, from a given class of records, may be considered equal to that from URR for each oscillation period in the considered range. Hypothesis tests were performed for both peak and cyclic EDPs. Regarding peak response inelastic displacement $Sd_{R=i}$

(i=1,2,4,6,10) was chosen as the variable to test and it was considered to have lognormal distribution. What found for the inelastic displacement is valid also for D_{kin}, see Equation (4), considering the *constant strength approach* adopted. Regarding cyclic response, N_e+1 was chosen as the variable to test, again, with lognormal distribution[4].
The null hypothesis to check was whether median EDPs for any class of records was equal (null hypothesis) or not (alternate hypothesis) to that from URR. To this aim a two-tails Aspin-Welch test [31] was preferred with respect to the standard *T-Student* test, as the former does not require the assumption of equal, yet still unknown, variances of populations originating the samples, which would be an unreasonable assumption given the natures of the compared record classes.
The test statistic employed is reported in Equation (6) in which z_x and z_y are the sample means, s_x and s_y are the sample standard deviations and n and m are the samples sizes (in this case always equal to 28). The test statistic, under the null hypothesis, has an approximate Student-T distribution with a number of degrees of freedom given by Satterthwaite's approximation [32].

$$t = \frac{z_x - z_y}{\sqrt{\frac{s_x^2}{n} + \frac{s_y^2}{m}}} \qquad (6)$$

Because URR were assumed as a benchmark, a preliminary test was performed to check if it was possible to reject the null hypothesis in terms of elastic displacement first. Table 2 presents *p-values* divided per period, bold are the rejection cases assuming a 95% significance level; i.e., choosing I-type risk (α) equal to 0.05. Periods values reported in the hypothesis tests tables are step by 0.2s for the sake of brevity.

Table 2 Aspin – Welch test results for elastic displacements, *p-values* lower than 0.05 are reported in bold.

Period (s)		*0.2*	*0.4*	*0.6*	*0.8*	*1*	*1.2*	*1.4*	*1.6*	*1.8*	*2*
Compared		*R = 1*									
URR	*SF12*	0.882	0.328	0.178	0.308	0.382	0.379	0.467	0.676	0.647	0.699
URR	*SF5*	0.997	0.390	0.243	0.682	0.666	0.462	0.361	0.323	0.282	0.281
URR	*RSPM*	0.895	0.172	0.271	0.312	0.278	0.249	0.229	0.273	0.295	0.194
URR	*Belf*	0.878	0.183	0.230	0.362	0.308	0.258	0.215	0.281	0.323	0.229
URR	*Simq*	0.826	0.162	0.237	0.284	0.246	0.189	0.192	0.195	0.220	0.172

Table 3, Table 4 and Table 5 show the test results for different R values (2,4,6,10) and for EPH, EPP and ESD SDOF models, respectively. Results presented in Table 3 show that there are no rejections with respect to URR records at any reduction factor. Results in term of displacements are qualitatively similar to EPH with no rejections (Table 4). From Table 5 it is recognizable a number of rejections in comparing real and artificial accelerograms. It is worth to note that, in this case, the results relative to high R values (6,10) are affected by the fact that ductility demand exceeds the *ductility limit* and rejections associated to Simqke records indicate displacements significantly higher than those of real record, see Figure 8c and Figure 8d.
Table 6, Table 7 and Table 8 show test results for different R values on equivalent number of cycles respectively for EPH, EPP and ESD systems. As it was expected, considering the results in section 4.3, there are a large number of rejections for this EDP for all kinds of SDOF models, especially for Belfagor and Simqke accelerograms. RSPMatch records do not lead to a significant number of rejections.

[4] Distribution assumptions were checked with the Lilliefors test [30], and could not be rejected at 95% significance level.

Table 3. Aspin-Welch test results for inelastic displacements of EPH system, *p-values* lower than 0.05 are reported in bold.

Period (s)		*0.2*	*0.4*	*0.6*	*0.8*	*1*	*1.2*	*1.4*	*1.6*	*1.8*	*2*
Compared		*R = 2*									
URR	*SF12*	0.903	0.505	0.533	0.822	0.618	0.430	0.728	0.800	0.392	0.352
URR	*SF5*	0.777	0.528	0.564	0.932	0.690	0.652	0.360	0.276	0.248	0.220
URR	*RSPM*	0.914	0.521	0.534	0.737	0.381	0.362	0.250	0.270	0.183	0.119
URR	*Belf*	0.990	0.603	0.673	0.540	0.841	0.918	0.997	0.793	0.566	0.389
URR	*Simq*	0.623	0.089	0.227	0.638	0.643	0.309	0.320	0.211	0.230	0.057
Compared		*R = 4*									
URR	*SF12*	0.389	0.498	0.920	0.578	0.421	0.389	0.398	0.355	0.269	0.292
URR	*SF5*	0.279	0.830	0.512	0.966	0.530	0.362	0.255	0.162	0.134	0.166
URR	*RSPM*	0.813	0.723	0.495	0.946	0.590	0.599	0.387	0.218	0.140	0.124
URR	*Belf*	0.761	0.884	0.420	0.466	0.617	0.782	0.980	0.956	0.995	0.991
URR	*Simq*	0.803	0.530	0.826	0.932	0.715	0.496	0.170	0.165	0.113	0.069
Compared		*R = 6*									
URR	*SF12*	0.358	0.736	0.768	0.435	0.612	0.459	0.354	0.423	0.426	0.516
URR	*SF5*	0.366	0.956	0.853	0.469	0.661	0.446	0.288	0.177	0.158	0.228
URR	*RSPM*	0.891	0.927	0.960	0.969	0.730	0.426	0.244	0.179	0.190	0.319
URR	*Belf*	0.830	0.793	0.867	0.378	0.559	0.830	0.908	0.945	0.998	0.849
URR	*Simq*	0.745	0.846	0.797	0.909	0.787	0.487	0.323	0.206	0.137	0.318
Compared		*R = 10*									
URR	*SF12*	0.460	0.562	0.517	0.587	0.656	0.607	0.479	0.600	0.679	0.880
URR	*SF5*	0.545	0.825	0.578	0.477	0.534	0.436	0.260	0.295	0.365	0.325
URR	*RSPM*	0.764	0.923	0.977	0.787	0.520	0.478	0.266	0.316	0.461	0.554
URR	*Belf*	0.290	0.155	0.142	0.148	0.503	0.821	0.690	0.792	0.894	0.781
URR	*Simq*	0.788	0.657	0.601	0.581	0.872	0.754	0.410	0.417	0.399	0.327

Table 4. Aspin-Welch test results for inelastic displacements of EPP system, *p-values* lower than 0.05 are reported in bold.

Period (s)		*0.2*	*0.4*	*0.6*	*0.8*	*1*	*1.2*	*1.4*	*1.6*	*1.8*	*2*
Compared		*R = 2*									
URR	*SF12*	0.620	0.690	0.826	0.630	0.610	0.585	0.730	0.669	0.475	0.528
URR	*SF5*	0.878	0.710	0.824	0.928	0.749	0.712	0.350	0.289	0.270	0.230
URR	*RSPM*	0.541	0.770	0.835	0.822	0.483	0.590	0.429	0.365	0.164	0.131
URR	*Belf*	0.543	0.815	0.645	0.475	0.638	0.890	0.973	0.757	0.664	0.644
URR	*Simq*	0.976	0.633	0.789	0.625	0.896	0.787	0.608	0.738	0.457	0.388
Compared		*R = 4*									
URR	*SF12*	0.366	0.394	0.613	0.516	0.507	0.520	0.321	0.329	0.395	0.445
URR	*SF5*	0.490	0.680	0.805	0.741	0.494	0.407	0.260	0.204	0.193	0.212
URR	*RSPM*	0.591	0.626	0.699	0.816	0.677	0.433	0.238	0.185	0.152	0.193
URR	*Belf*	0.424	0.768	0.314	0.247	0.718	0.773	0.741	0.730	0.543	0.605
URR	*Simq*	0.350	0.911	0.783	0.365	0.735	0.895	0.612	0.324	0.360	0.404
Compared		*R = 6*									
URR	*SF12*	0.273	0.328	0.422	0.428	0.523	0.444	0.385	0.499	0.713	0.849
URR	*SF5*	0.574	0.831	0.633	0.396	0.436	0.362	0.237	0.202	0.256	0.298
URR	*RSPM*	0.669	0.919	0.642	0.683	0.485	0.287	0.207	0.178	0.222	0.239
URR	*Belf*	0.878	0.559	0.432	0.592	0.804	0.649	0.774	0.791	0.713	0.671
URR	*Simq*	0.465	0.966	0.693	0.667	0.846	0.766	0.499	0.453	0.528	0.487
Compared		*R = 10*									
URR	*SF12*	0.195	0.313	0.346	0.488	0.504	0.487	0.616	0.868	0.977	0.975
URR	*SF5*	0.494	0.508	0.314	0.372	0.377	0.253	0.254	0.402	0.465	0.468
URR	*RSPM*	0.489	0.508	0.494	0.420	0.291	0.218	0.214	0.364	0.487	0.404
URR	*Belf*	0.487	0.415	0.720	0.533	0.637	0.795	0.957	0.944	0.948	0.941
URR	*Simq*	0.503	0.967	0.898	0.951	0.908	0.589	0.498	0.549	0.542	0.452

Table 5. Aspin-Welch test results for inelastic displacements of ESD system, *p-values* lower than 0.05 are reported in bold.

Period (s)		*0.2*	*0.4*	*0.6*	*0.8*	*1.0*	*1.2*	*1.4*	*1.6*	*1.8*	*2.0*
Compared		*R = 2*									
URR	*SF12*	0.491	0.981	0.914	0.654	0.761	0.747	0.864	0.709	0.545	0.552
URR	*SF5*	0.163	0.976	0.692	0.909	0.795	0.839	0.326	0.292	0.278	0.228
URR	*RSPM*	0.072	0.849	0.874	0.672	0.725	0.868	0.571	0.426	0.210	0.156
URR	*Belf*	0.080	0.882	0.434	0.416	0.438	0.648	0.772	0.879	0.845	0.738
URR	*Simq*	0.208	0.955	0.629	0.559	0.670	0.975	0.744	0.853	0.579	0.432
Compared		*R = 4*									
URR	*SF12*	**0.013**	0.796	0.883	0.460	0.457	0.475	0.454	0.420	0.496	0.600
URR	*SF5*	**0.046**	0.881	0.835	0.483	0.365	0.306	0.210	0.177	0.209	0.242
URR	*RSPM*	**0.010**	0.787	0.467	0.553	0.725	0.462	0.233	0.214	0.226	0.200
URR	*Belf*	**0.003**	0.212	0.364	0.443	0.845	0.743	0.786	0.714	0.481	0.513
URR	*Simq*	**0.000**	0.729	0.818	0.460	0.660	0.850	0.585	0.429	0.426	0.469
Compared		*R = 6*									
URR	*SF12*	**0.001**	**0.011**	0.112	0.474	0.520	0.444	0.590	0.909	0.529	0.661
URR	*SF5*	**0.004**	0.103	0.282	0.275	0.311	0.224	0.203	0.274	0.488	0.510
URR	*RSPM*	**0.027**	**0.036**	0.140	0.319	0.207	0.260	0.231	0.269	0.490	0.469
URR	*Belf*	**0.001**	**0.011**	**0.030**	0.210	0.556	0.750	0.502	0.535	0.271	0.270
URR	*Simq*	**0.000**	**0.000**	**0.000**	**0.002**	**0.017**	0.055	0.168	0.314	0.615	0.598
Compared		*R = 10*									
URR	*SF12*	**0.047**	**0.007**	0.114	0.114	0.253	0.275	0.366	0.564	0.650	0.930
URR	*SF5*	**0.012**	0.062	0.207	0.281	0.187	0.147	0.365	0.524	0.461	0.576
URR	*RSPM*	0.135	**0.015**	0.335	0.188	0.158	**0.046**	0.100	0.280	0.344	0.374
URR	*Belf*	**0.011**	**0.002**	0.079	0.278	0.337	0.258	0.621	0.948	0.612	0.439
URR	*Simq*	**0.005**	**0.000**	**0.002**	**0.004**	**0.002**	**0.003**	**0.008**	**0.027**	**0.038**	**0.042**

Table 6. Aspin-Welch test results for equivalent number of cycles of EPH system, *p-values* lower than 0.05 are reported in bold.

Period (s)		*0.2*	*0.4*	*0.6*	*0.8*	*1*	*1.2*	*1.4*	*1.6*	*1.8*	*2*
Compared		*R = 2*									
URR	*SF12*	0.812	**0.028**	**0.037**	**0.012**	0.101	0.224	**0.044**	**0.046**	0.587	0.658
URR	*SF5*	0.992	0.166	0.114	0.439	0.365	0.128	**0.043**	0.170	0.243	0.142
URR	*RSPM*	0.427	**0.003**	**0.033**	**0.018**	0.389	0.161	**0.036**	**0.026**	0.051	**0.015**
URR	*Belf*	**0.040**	**0.000**	**0.001**	**0.024**	**0.001**	**0.002**	**0.000**	**0.000**	**0.001**	**0.001**
URR	*Simq*	**0.000**	**0.000**	**0.000**	**0.000**	**0.000**	**0.002**	**0.000**	**0.000**	**0.000**	**0.001**
Compared		*R = 4*									
URR	*SF12*	0.597	0.071	**0.010**	**0.021**	0.116	0.074	0.177	0.307	0.593	0.402
URR	*SF5*	0.339	0.303	**0.024**	**0.036**	0.167	0.199	**0.045**	0.131	0.157	0.146
URR	*RSPM*	0.526	0.078	**0.010**	0.173	0.298	**0.043**	**0.020**	**0.028**	**0.044**	**0.047**
URR	*Belf*	**0.004**	**0.000**	**0.000**	**0.000**	**0.000**	**0.000**	**0.000**	**0.000**	**0.000**	**0.000**
URR	*Simq*	**0.000**	**0.000**	**0.000**	**0.000**	**0.000**	**0.000**	**0.000**	**0.000**	**0.000**	**0.000**
Compared		*R = 6*									
URR	*SF12*	0.781	**0.033**	*0.019*	**0.044**	**0.019**	0.139	0.158	0.193	0.459	0.195
URR	*SF5*	0.641	0.212	0.060	0.207	**0.023**	0.091	**0.045**	0.069	0.250	0.129
URR	*RSPM*	0.294	0.133	0.092	0.156	0.085	0.087	**0.046**	0.056	0.105	**0.020**
URR	*Belf*	**0.000**	**0.000**	**0.000**	**0.000**	**0.000**	**0.000**	**0.000**	**0.000**	**0.001**	**0.000**
URR	*Simq*	**0.000**	**0.000**	**0.000**	**0.000**	**0.000**	**0.000**	**0.000**	**0.000**	**0.000**	**0.000**
Compared		*R = 10*									
URR	*SF12*	0.408	**0.049**	0.059	**0.022**	**0.026**	0.070	0.180	0.148	0.202	0.081
URR	*SF5*	0.891	0.252	0.231	0.140	0.072	0.083	0.221	0.153	0.162	0.192
URR	*RSPM*	0.314	0.129	0.092	0.071	0.098	**0.033**	0.111	0.061	**0.029**	**0.013**
URR	*Belf*	**0.000**	**0.000**	**0.000**	**0.000**	**0.000**	**0.000**	**0.001**	**0.001**	**0.000**	**0.000**
URR	*Simq*	**0.000**	**0.000**	**0.000**	**0.000**	**0.000**	**0.000**	**0.000**	**0.000**	**0.000**	**0.000**

Table 7. Aspin-Welch test results for equivalent number of cycles of EPP system, *p-values* lower than 0.05 are reported in bold.

Period (s)		*0.2*	*0.4*	*0.6*	*0.8*	*1*	*1.2*	*1.4*	*1.6*	*1.8*	*2*
Compared		*R = 2*									
URR	*SF12*	0.571	**0.004**	**0.011**	**0.032**	0.092	0.051	0.054	0.180	0.394	0.322
URR	*SF5*	0.221	**0.025**	**0.009**	0.121	0.077	**0.013**	**0.010**	0.107	0.193	0.093
URR	*RSPM*	**0.047**	**0.002**	**0.003**	**0.020**	0.069	**0.007**	**0.001**	**0.002**	**0.008**	**0.001**
URR	*Belf*	**0.000**	**0.000**	**0.000**	**0.000**	**0.000**	**0.000**	**0.000**	**0.000**	**0.000**	**0.000**
URR	*Simq*	**0.000**	**0.000**	**0.000**	**0.000**	**0.000**	**0.000**	**0.000**	**0.000**	**0.000**	**0.000**
Compared		*R = 4*									
URR	*SF12*	0.396	0.060	**0.047**	**0.028**	0.065	0.051	0.250	0.292	0.500	0.196
URR	*SF5*	0.787	0.195	**0.020**	**0.030**	**0.061**	0.068	**0.018**	0.084	0.160	0.129
URR	*RSPM*	0.463	0.284	**0.038**	**0.021**	0.059	**0.034**	**0.023**	**0.027**	**0.048**	**0.020**
URR	*Belf*	**0.000**	**0.000**	**0.000**	**0.000**	**0.000**	**0.000**	**0.000**	**0.000**	**0.000**	**0.000**
URR	*Simq*	**0.000**	**0.000**	**0.000**	**0.000**	**0.000**	**0.000**	**0.000**	**0.000**	**0.000**	**0.000**
Compared		*R = 6*									
URR	*SF12*	0.345	0.149	0.061	0.126	0.200	0.236	0.254	0.169	0.116	**0.031**
URR	*SF5*	0.413	0.092	0.070	0.194	0.105	0.091	0.109	0.142	0.278	0.114
URR	*RSPM*	0.482	0.137	0.221	0.082	0.101	0.127	0.114	0.125	0.201	0.075
URR	*Belf*	**0.000**	**0.000**	**0.000**	**0.000**	**0.000**	**0.000**	**0.000**	**0.000**	**0.000**	**0.000**
URR	*Simq*	**0.000**	**0.000**	**0.000**	**0.000**	**0.000**	**0.000**	**0.000**	**0.000**	**0.000**	**0.000**
Compared		*R = 10*									
URR	*SF12*	0.463	0.131	0.230	0.144	0.282	0.359	0.347	0.059	0.047	0.027
URR	*SF5*	0.320	0.165	0.369	0.231	0.259	0.537	0.744	0.240	0.213	0.125
URR	*RSPM*	0.731	0.514	0.176	0.143	0.382	0.494	0.770	0.210	0.124	0.120
URR	*Belf*	**0.000**	**0.000**	**0.000**	**0.000**	**0.000**	**0.000**	**0.004**	**0.002**	**0.006**	**0.006**
URR	*Simq*	**0.000**	**0.000**	**0.000**	**0.000**	**0.000**	**0.000**	**0.000**	**0.000**	**0.000**	**0.000**

Table 8. Aspin-Welch test results for equivalent number of cycles of ESD system, *p-values* lower than 0.05 are reported in bold.

Period (s)		*0.2*	*0.4*	*0.6*	*0.8*	*1.0*	*1.2*	*1.4*	*1.6*	*1.8*	*2.0*
Compared		*R = 2*									
URR	*SF12*	0.116	**0.002**	**0.009**	**0.034**	0.076	**0.046**	0.051	0.189	0.347	0.337
URR	*SF5*	**0.022**	**0.013**	**0.007**	0.105	0.058	**0.007**	**0.015**	0.125	0.219	0.105
URR	*RSPM*	**0.002**	**0.001**	**0.001**	**0.015**	**0.047**	**0.004**	**0.001**	**0.002**	**0.006**	**0.002**
URR	*Belf*	**0.000**	**0.000**	**0.000**	**0.000**	**0.000**	**0.000**	**0.000**	**0.000**	**0.000**	**0.000**
URR	*Simq*	**0.000**	**0.000**	**0.000**	**0.000**	**0.000**	**0.000**	**0.000**	**0.000**	**0.000**	**0.000**
Compared		*R = 4*									
URR	*SF12*	0.094	**0.028**	**0.035**	0.084	0.131	0.063	0.135	0.227	0.350	0.108
URR	*SF5*	0.263	**0.036**	**0.007**	0.084	0.141	0.124	**0.033**	0.154	0.195	0.140
URR	*RSPM*	**0.002**	0.108	**0.018**	**0.007**	0.076	0.056	**0.037**	**0.043**	**0.048**	**0.041**
URR	*Belf*	0.464	**0.000**	**0.000**	**0.000**	**0.000**	**0.000**	**0.000**	**0.000**	**0.000**	**0.000**
URR	*Simq*	0.312	**0.000**	**0.000**	**0.000**	**0.000**	**0.000**	**0.000**	**0.000**	**0.000**	**0.000**
Compared		*R = 6*									
URR	*SF12*	**0.020**	0.167	0.408	0.065	0.168	0.218	0.095	**0.028**	**0.003**	**0.003**
URR	*SF5*	0.105	0.770	0.345	0.422	0.418	0.389	0.209	0.127	0.151	0.053
URR	*RSPM*	0.067	0.267	0.592	0.417	0.905	0.382	0.235	0.183	0.182	0.065
URR	*Belf*	0.989	0.181	0.063	**0.009**	**0.007**	**0.000**	**0.000**	**0.000**	**0.000**	**0.000**
URR	*Simq*	0.829	0.368	0.103	**0.036**	**0.015**	**0.004**	**0.001**	**0.000**	**0.000**	**0.000**
Compared		*R = 10*									
URR	*SF12*	0.417	0.079	0.707	0.530	0.390	0.675	0.630	0.272	0.325	0.070
URR	*SF5*	0.947	0.652	0.735	0.439	0.769	0.782	0.896	0.306	0.394	0.133
URR	*RSPM*	0.964	**0.023**	0.829	0.736	0.963	0.394	0.345	0.910	0.736	0.362
URR	*Belf*	0.085	0.662	**0.033**	**0.007**	0.073	0.330	0.329	0.062	**0.024**	**0.005**
URR	*Simq*	**0.003**	0.508	0.337	0.088	0.382	0.497	0.457	0.153	0.118	**0.042**

For ESD models (Table 8) rejections at all periods indicate always an overestimation of artificial records. The number of rejections tends to reduce at high nonlinearity levels. In fact, in the previous section it was observed that, when ductility demand exceeds the *ductility limit*, the equivalent number of cycles tends to be similar for all six classes. Scaled real records present only a few rejections with respect to URR records.

6 CONCLUSIONS

In this work different ways to achieve spectrum matching record sets were compared in terms of post-elastic seismic peak and cyclic responses. This was pursued considering SDOFs with three different force-displacement backbones and hysteretic rules at different nonlinearity levels. The ductility and equivalent number of cycles response of 240 systems were analyzed with respect to six classes of records: real unscaled, real with moderate linear scaling factor, real with significant linear scaling factor, real adjusted with wavelets, and two different types of artificial records.
The *life-safety* design elastic spectrum, for a case study site in southern Italy, was considered; all the classes of records match it on average or by means of individual records.
Results indicate that the linearly scaled records do not show any-systematic trend with respect to the unscaled records' results independently of the backbone and response parameters, suggesting that scaling is a legitimate technique, as many studies point out, if the spectral shape is controlled.
RSPMatch2005 wavelet-adjustment procedure shows small, if any, bias in terms of peak and cyclic responses. Conversely, both classes of artificial records, but especially non-stationary accelerograms, in some cases seem to underestimate peak demand (ductility). Artificial records, especially those stationary, gave strong cyclic response overestimation (at least until ductility demand let the hysteresis to reach the residual strength of the backbone, although this is more a modeling issue).
Hypothesis tests were carried out with the aim of assessing quantitatively how much these results are significant. Tests have shown a statistical significance of the bias of artificial records only in terms of cyclic response. Regarding peak response, test results suggest that underestimation of artificial records with respect to unscaled real records does not have statistical significance. In fact, it is significant only in the case of the degrading systems (ESD) at high nonlinearity levels, when modeling hypotheses have a strong influence.
It is to note that, as it is well known, the cyclic response overestimation could have been predicted by some integral parameters of ground motion, which, if appropriate hazard analysis tool is available, could be used as an additional criterion for record selection especially in those cases when cyclic behavior has an important role in determining the seismic performances.

REFERENCES

[1] Iervolino I., Maddaloni G., Cosenza E. 2008. Eurocode 8 compliant real record sets for seismic analysis of structures. *Journal of Earthquake Engineering*, 12(1), 54-90.

[2] Comité Européen de Normalisation, 2003. *Eurocode8, Design of Structures for earthquake resistance – Part1: General rules, seismic actions and rules for buildings*. EN 1998-1, CEN, Brussels.

[3] Bommer J.J, Acevedo A.B., 2004. *The use of real earthquake accelerograms as input to dynamic analysis*. Journal of Earthquake Engineering. 8(Special Issue I), 43-91.

[4] CS.LL.PP; DM 14 Gennaio 2008: Norme tecniche per le costruzioni. *Gazzetta Ufficiale della Repubblica Italiana*, 29. 4/2/2008 (In Italian).

[5] Convertito V., Iervolino I., Herrero A., 2009. The importance of mapping the design earthquake: insights for southern Italy. *Bulletin of the Seismological Society of America*, 99(5), 2979–2991.

[6] Iervolino I., Maddaloni G., Cosenza E., 2009. A note on selection of time-histories for seismic analysis of bridges in Eurocode 8. *Journal of Earthquake Engineering*, 13(8), 1125–1152.

[7] Hancock J., Watson-Lamprey, J., Abrahamson N.A., Bommer J.J., Markatis A., McCoy E., Mendis E., 2006. An improved method of matching response spectra of recorded earthquake ground motion using wavelets. *Journal of Earthquake Engineering*, 10(Special Issue I), 67-89.

[8] Iervolino I., Cornell C.A., 2005 Record selection for nonlinear seismic analysis of structures. *Earthquake Spectra*, 21(3), 685-713.

[9] Schwab P., Lestuzzi P., 2007. Assessment of the seismic nonlinear behaviour of ductile wall structures due to synthetic earthquakes. *Bulletin of Earthquake Engineering*, 5, 67-84.

[10] Iervolino I., Manfredi G., Cosenza E., 2006. Ground motion duration effects on nonlinear seismic response. *Earthquake Engineering and Structural Dynamics*, 30, 485–499.

[11] Manfredi G., 2001. Evaluation of seismic energy demand. *Earthquake Engineering and Structural Dynamics*, 35, 21–38.

[12] Esposito M., 2009. Accelerogrammi spettrocompatibili per la progettazione delle strutture: valutazione comparativa della risposta sismica. Dipartimento di Ingegneria Strutturale, Università degli Studi di Napoli Federico II. Graduation Thesis. Advisors: E. Cosenza, I. Iervolino, F. De Luca. Available at http://wpage.unina.it/iuniervo/ (in Italian)

[13] Iervolino I., Galasso C., Cosenza E., 2009. REXEL: computer aided record selection for code-based seismic structural analysis. *Bulletin of Earthquake Engineering*. 8:339-362.

[14] Baker J.W., Cornell C.A., 2006. Spectral shape, epsilon and record selection. *Earthquake Engineering and Structural Dynamics*, 35(9), 1077–1095.

[15] Hancock J., Bommer J.J., Stafford P.J., 2008. Number of scaled and matched accelerograms required for inelastic dynamic analyses. *Earthquake Engineering and Structural Dynamics*, 37(14), 1585-1607.

[16] PEER ground motion selection and modification working group – Haselton C.B., editor, 2009. Evaluation of Ground Motion selection methods: prediction median interstory drift response of buildings. PEER report 2009/01 available at http://peer.berkeley.edu/publications/peer_reports/reports_2009.

[17] Abrahamson N.A., 1992. Non-stationary spectral matching. *Seismological research letters*. 63(1), 30.

[18] Grant D.N., Greening P.D., Taylor M.L. and Ghosh B, 2008. Seed record selection for spectral matching with RSPMatch2005. Proceedings of *14thWorld Conference on Earthquake Engineering*, October 12-17, Beijing, China.

[19] Pinto P.E., Giannini R., Franchin P., 2004. *Seismic reliability analysis of structures*. IUSS Press, Pavia, Italy.

[20] Mucciarelli M., Spinelli A., Pacor F., 2004. Un programma per la generazione di accelerogrammi sintetici "fisici" adeguati alla nuova normativa. XI *Convegno ANIDIS*, *"L'Ingegneria Sismica in Italia"*. January 25-29, Genoa, Italy.

[21] Sabetta, F., Pugliese, A., 1996. Estimation of response spectra and simulation of non stationary earthquake ground motions. *Bulletin of the Seismological Society of America*, 86(2), 337-52.

[22] Gasparini D.A., Vanmarke E.H., 1976. *Simulated earthquake motions compatible with prescribed response* spectra. MIT civil engineering research report R76-4. Massachusetts Institute of Technology, Cambridge, MA.

[23] Cosenza E., Manfredi G., Ramasco R., 1993. The Use of Damage Functionals in Earthquake-Resistant Design: a Comparison Among Different Procedures. Earthquake Engineering and Structural Dynamics, 22(10), 855-868.

[24] Iervolino I. , Giorgio M., Galasso C., Manfredi G.; 2008. Prediction relationships for a vector valued ground motion intensity measure accounting for cumulative damage potential, 14th World Conference on Earthquake Engineering, Beijing, China, October 12-17.

[25] Iervolino I., Galasso C., Manfredi G., 2009. Conditional hazard analysis for secondary intensity measures. *Bulletin of the Seismological Society of America*. (submitted).

[26] Clough R.W., Johnston S.B., 1966 Effect of stiffness degradation on earthquake ductility requirements. Proceedings of *Japan Earthquake Engineering Symposium*, Tokyo, Japan.

[27] Takeda T., Sozen M.A., Nielsen N.N., 1970. Reinforced concrete response to simulated earthquakes, *Journal of Structural Engineering Division*, ASCE, 96(12), 2557–2573.

[28] Bazzurro P., Luco N., 2004. *Post-elastic response of structures to synthetic ground motions*. Report for Pacific Earthquake Engineering Research (PEER) Center Lifelines Program Project 1G00 Addenda. CA, US.

[29] Benjamin J., Cornell A., 1970. *Probability, statistics and decision for civil engineers*, Mc Graw-Hill, NY, USA.

[30] Lilliefors H.W., 1967. On the Komogorov-Smirnov test for normality with mean and variance unknown. *Journal of the American Statistical Association*, 62, 399-402.

[31] Welch B. L., 1938. The significance of the difference between two means when the population variances are unequal. *Biometrika*, 29, 350-62.

[32] Satterthwaite F.E., 1941. Synthesis of variance. *Psychometrika*, 6(5), 309-316.

APPENDIX

In this appendix data regarding real records selected are reported. Table A1 collects, for the URR class, records no. and event no. according to European Strong Motion Database. Table A2 and A3 collect the same information for SF5 and SF12 classes, respectively (in these two tables the scaling factor applied to each single record is also reported). In the tables, x and y represent the two horizontal components of the record.

Table A1. Information according to ESD for URR records.

Set	*Waveform no.*	*Earthquake no.*	*Earthquake Name*	*Date*	*Mw*	*Fault Mechanism*	R_e *(km)*
I	365y	175	Lazio Abruzzo	07/05/1984	5.9	normal	5
	4674x	1635	South Iceland	17/06/2000	6.5	strike slip	5
	4675y	1635	South Iceland	17/06/2000	6.5	strike slip	13
	4675x	1635	South Iceland	17/06/2000	6.5	strike slip	13
	6326y	2142	South Iceland (aftershock)	21/06/2000	6.4	strike slip	14
	6332x	2142	South Iceland (aftershock)	21/06/2000	6.4	strike slip	6
	6335x	2142	South Iceland (aftershock)	21/06/2000	6.4	strike slip	15
II	182y	87	Tabas	16/09/1978	7.3	oblique	12
	242x	115	Valnerina	19/09/1979	5.8	normal	5
	242y	115	Valnerina	19/09/1979	5.8	normal	5
	1231x	472	Izmit	17/08/1999	7.6	strike slip	9
	1231y	472	Izmit	17/08/1999	7.6	strike slip	9
	3802x	1226	SE of Tirana	09/01/1988	5.9	thrust	7
	7142y	2309	Bingol	01/05/2003	6.3	strike slip	14
III	234x	108	Montenegro (aftershock)	24/05/1979	6.2	thrust	30
	287x	146	Campano Lucano	23/11/1980	6.9	normal	23
	287y	146	Campano Lucano	23/11/1980	6.9	normal	23
	290x	146	Campano Lucano	23/11/1980	6.9	normal	32
	665x	286	Umbria Marche	26/09/1997	6	normal	21
	6500x	497	Duzce 1	12/11/1999	7.2	oblique	23
	7156x	2313	Firuzabad	20/06/1994	5.9	strike slip	21

	55x	34	Friuli	06/05/1976	6.5	thrust	23
	198x	93	Montenegro	15/04/1979	6.9	thrust	21
	198y	93	Montenegro	15/04/1979	6.9	thrust	21
IV	4678x	1635	South Iceland	17/06/2000	6.5	strike slip	32
	6342x	2142	South Iceland (aftershock)	21/06/2000	6.4	strike slip	20
	6342y	2142	South Iceland (aftershock)	21/06/2000	6.4	strike slip	20
	7187x	2322	Avej	22/06/2002	6.5	thrust	28

Table A2. Information according to ESD and SF factors for SF5 records.

Set	*Waveform no.*	*Earthquake no.*	*Earthquake Name*	*Date*	*Mw*	*Mechanism*	*R_e (km)*	*SF*
	234y	108	Montenegro (aftershock)	24/05/1979	6.2	thrust	30	2.499
	292x	146	Campano Lucano	23/11/1980	6.9	normal	25	3.206
	292y	146	Campano Lucano	23/11/1980	6.9	normal	25	3.207
I	368x	175	Lazio Abruzzo	07/05/1984	5.9	normal	22	3.000
	410x	189	Golbasi	05/05/1986	6	oblique	29	4.918
	5272x	1338	Mt. Vatnafjoll	25/05/1987	6	oblique	24	5.848
	6262y	1635	South Iceland	17/06/2000	6.5	strike slip	31	2.848
	182y	87	Tabas	16/09/1978	7.3	oblique	12	0.499
	182x	87	Tabas	16/09/1978	7.3	oblique	12	0.568
	471y	227	Vrancea	30/05/1990	6.9	thrust	6	8.037
II	1243x	473	Izmit (aftershock)	13/09/1999	5.8	oblique	15	2.640
	4674	1635	South Iceland	17/06/2000	6.5	strike slip	5	0.604
	4675x	1635	South Iceland	17/06/2000	6.5	strike slip	13	1.459
	7142y	2309	Bingol	01/05/2003	6.3	strike slip	14	0.646
	55x	34	Friuli	06/05/1976	6.5	thrust	23	0.539
	55y	34	Friuli	06/05/1976	6.5	thrust	23	0.608
	6327y	2142	South Iceland (aftershock)	21/06/2000	6.4	strike slip	24	3.241
III	6331y	2142	South Iceland (aftershock)	21/06/2000	6.4	strike slip	22	4.881
	6331x	2142	South Iceland (aftershock)	21/06/2000	6.4	strike slip	22	3.673
	6333x	2142	South Iceland (aftershock)	21/06/2000	6.4	strike slip	28	9.450
	7187x	2322	Avej	22/06/2002	6.5	thrust	28	0.431

IV	473y	228	Vrancea	31/05/1990	6.3	thrust	7	21.822
	3802x	1226	SE of Tirana	09/01/1988	5.9	thrust	7	1.693
	6326y	2142	South Iceland (aftershock)	21/06/2000	6.4	strike slip	14	1.649
	6332x	2142	South Iceland (aftershock)	21/06/2000	6.4	strike slip	6	0.363
	6335y	2142	South Iceland (aftershock)	21/06/2000	6.4	strike slip	15	1.664
	6335x	2142	South Iceland (aftershock)	21/06/2000	6.4	strike slip	15	1.510
	6349y	2142	South Iceland (aftershock)	21/06/2000	6.4	strike slip	5	0.229

Table A3. Information according to ESD and SF factors for SF12 records.

Set	*Waveform no.*	*Earthquake no.*	*Earthquake Name*	*Date*	*Mw*	*Mechanism*	*R_e (km)*	*SF*
I	169x	80	Calabria	11/03/1978	5.2	normal	10	2.539
	382y	176	Lazio Abruzzo (aftershock)	11/05/1984	5.5	normal	16	12.811
	383x	176	Lazio Abruzzo (aftershock)	11/05/1984	5.5	normal	14	9.502
	5078x	1464	Mt. Hengill Area	04/06/1998	5.4	strike slip	18	14.219
	5085x	1464	Mt. Hengill Area	04/06/1998	5.4	strike slip	15	15.714
	5086x	1464	Mt. Hengill Area	04/06/1998	5.4	strike slip	15	8.396
	5090x	1464	Mt. Hengill Area	04/06/1998	5.4	strike slip	18	6.128
II	95y	52	Friuli (aftershock)	17/06/1976	5.2	oblique	26	21.301
	95x	52	Friuli (aftershock)	17/06/1976	5.2	oblique	26	19.028
	642y	292	Umbria Marche (aftershock)	14/10/1997	5.6	normal	23	3.049
	1891y	651	Kranidia	25/10/1984	5.5	?	23	7.382
	1893y	652	Near SW coast of Peloponnes	10/12/1987	5.2	?	30	11.385
	5089y	1464	Mt. Hengill Area	04/06/1998	5.4	strike slip	23	11.917
	5895y	1932	Arnissa	09/07/1984	5.2	normal	30	17.543
III	847x	363	Umbria Marche (aftershock)	26/03/1998	5.4	oblique	41	8.620
	1884y	229	Filippias	16/06/1990	5.5	thrust	43	16.711
	1899x	657	Gulf of Kiparissiakos	07/09/1985	5.4	oblique	37	9.182
	1994x	645	Skydra-Edessa	18/02/1986	5.3	?	31	18.973
	4560y	1387	Bovec	12/04/1998	5.6	strike slip	38	19.425
	5087x	1464	Mt. Hengill Area	04/06/1998	5.4	strike slip	32	28.143
	7089x	2290	Pasinler	10/07/2001	5.4	strike slip	32	9.833

IV[5]	410x	189	Golbasi	05/05/1986	6	oblique	29	5.918
	471y	227	Vrancea	30/05/1990	6.9	thrust	6	8.737
	473y	228	Vrancea	31/05/1990	6.3	thrust	7	19.322
	1243x	473	Izmit (aftershock)	13/09/1999	5.8	oblique	15	3.237
	5272x	1338	Mt. Vatnafjoll	25/05/1987	6	oblique	24	10.848
	6761y	2222	Vrancea	30/08/1986	7.2	thrust	49	1.439
	6761x	2222	Vrancea	30/08/1986	7.2	thrust	49	1.100

[5] "Manually" selected and scaled.